Defect Structure in Nickel Electrodeposits

S. Nakahara* and E. C. Felder

Bell Laboratories, Murray Hill, New Jersey 07974

ABSTRACT

A transmission electron microscope was used to study the influence of solution *p*H and temperature on the microstructure of nickel films obtained by electrodeposition. It was found that the solution *p*H and temperature affect the microstructure (density of dislocations and growth twins, and grain size) significantly. This microstructural modification was accompanied by a corresponding change in the ductility, current efficiency, and the hydrogen content of the deposits. These results can be rationalized by the strong tendency of nickel to be passivated by the adsorption of foreign species (hydrogen and hydroxide) present in the basic electrolyte during electrocrystallization. The marked dependence of such a passivation on the solution *p*H and temperature was found to support our conclusion that the observed changes are due to the adsorption and subsequent incorporation of hydrogen and hydroxide.

It is well documented (1-4) that the cathodic reduction of iron-group metals (Fe, Ni, and Co) is accompanied by high overpotential which is primarily caused by their strong tendency to be passivated by foreign species (hydrogen and hydroxide) present in the basic electrolyte. In other words, some kind of inhibition is already occurring even without the presence of deliberately added impurities, such as an addition agent. If this passivation is significantly high, an understanding of the effect of additional impurities on the microstructures is expected to become more difficult. Previous electrochemical studies (2-5) have shown that the degree of adsorption and subsequent incorporation of these species depends strongly on both solution *p*H and temperature. This adsorption generally decreases with increasing temperature.

The incorporation of these foreign species also modifies the microstructure. For example, microstructural modifications in one of the iron-group metals, cobalt, prepared at different *p*H ranges, are in fact a long-standing mystery in electrodeposition phenomena. A peculiar feature of cobalt deposits is that a high temperature fcc phase can be obtained from a low (<2.4) *p*H solution at ambient temperatures (6). Although this structural peculiarity was attributed (7) earlier to the formation of epitaxial fcc cobalt grown on fcc substrates, the fact that thick fcc cobalt films can still be obtained beyond the possible epitaxial thickness challenges this proposition. Nakahara and Mahajan (8) recently suggested that "fcc cobalt" can be produced by the simultaneous incorporation of hydrogen to form an "fcc cobalt hydride." Since this hydride is unstable at ambient temperatures, it decomposes into basic cobalt during the outdiffusion of hydrogen. As the cobalt hydride was assumed to form an fcc structure, a structural transformation from fcc hydride to hcp cobalt would induce faulting on the close-packed {111} planes. This mechanism indeed explains the observed highly faulted fcc cobalt obtained at low *p*H. In fact, highly faulted fcc cobalt is structurally equivalent to the hcp cobalt which can exist at ambient temperatures.

At high *p*H, on the other hand, stable hcp cobalt was obtained. In this case, the films contained a high density of inclusions in the form of colloidal cobalt hydroxide particles. These hydroxide inclusions are incorporated and were found to play a role as growth inhibitors. Hydroxide inclusions, therefore, helped refine the grain size.

These observations for cobalt deposits raise a question as to whether the other iron-group metals, for example, nickel, also exhibit a structural anomaly similar to that observed in cobalt electrodeposits. Although nickel involves a similar electrochemical behavior (4), there is no report that describes the possible existence of such an anomaly. Motivated by this question, we have made a transmission electron microscope (TEM) study on the microstructures of nickel electrodeposits obtained at various *p*H ranges and solution temperatures. As cobalt exhibits this unusual structural transformation (fcc → hcp) as a result of hydrogen inclusion and subsequent outdiffusion, it was thought interesting to observe the possible microstructural modifications of nickel by plating at low *p*H and low temperature ranges (see Fig. 1).

Experimental

The nickel bath composition used in this study consisted of 0.43M $NiSO_4 \cdot 6H_2O$ and 0.50M H_3BO_3. The *p*H of the freshly prepared bath was about 3.5. The bath *p*H was lowered by the addition of H_2SO_4 or raised by nickelous carbonate. Two *p*H values (1.5 and 5.8) and three solution temperatures (20°, 50°, and 100°C) were chosen here. All nickel films were deposited on a polished sheet of annealed OFHC copper at the current density of 5 mA/cm^2. The film thicknesses ranged from 1.2 to 45 μm.

In order to prepare TEM specimens, plated nickel films were first stripped off the copper substrates in a solution containing 500 g/liter CrO_3 and 50 g/liter

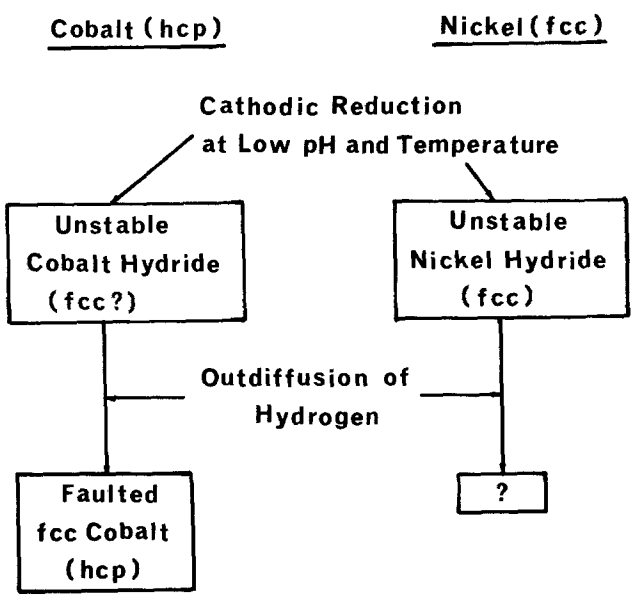

Fig. 1. A schematic diagram illustrating how iron-group metals (Co and Ni) undergo a structural change as a result of electrodeposition at low *p*H and low temperature.

* Electrochemical Society Active Member.
Key words: microstructure, solution *p*H, temperature.

H_2SO_4. Disks of 3 mm were then cut out of the stripped nickel foil and subsequently electropolished in a mixture of 860 cm^3 phosphoric acid, 50 cm^3 sulfuric acid, and 100g CrO_3. The electropolishing was carried out from both sides of the films, so that the microstructure away from substrate influence can be examined. TEM micrographs were obtained using a JEM 200 electron microscope operated at 200 kV. Inclusion images were taken using the defocus contrast technique (9).

Film ductility was measured using a novel ductility tester (10) developed recently in our laboratory. With this tester, film ductility is measured by pushing a spherical ball attached to the moving arm of a micrometer into the rigidly held nickel foil of approximately 1×1 cm^2 until the foil fractures. Since the distance between the initial contact with the ball and the final fracture is displayed digitally on the readout of the micrometer, it gives a measure of ductility in terms of the maximum percent elongation from a conversion table.

The measurements of the hydrogen content in nickel films were conducted by Gollob Analytical Service (Berkeley Heights, New Jersey) using a hot extraction method with a mass spectrometer readout.

Results

Nickel deposits obtained from a low pH (1.5) solution.—Figures 2 (a), (b), and (c) show the structures of nickel films deposited at 20°, 50°, and 100°C, respectively, in the low pH (1.5) solution. Hereafter, we call these films, A, B, and C, respectively. It is noted that the grain sizes vary considerably with solution temperature. The grain size of these films, A, B, and C, were found to be $0.5 \sim 1$, $6 \sim 20$, and $0.1 \sim 0.8$ μm, respectively. A careful examination of the microstructures further reveals that a high density of dislocations is present in film A, and numerous growth twins are visible in film C, which is, however, relatively free from dislocations.

In order to examine the nature of dislocations in film A, we have made a detailed analysis of these dislocation structures. Figure 3 indicates the presence of dislocations, for example, denoted by a symbol, D, inside the grain. The film is seen to have apparently undergone a plastic deformation. In some areas, these slip dislocations have formed a low angle grain boundary as seen in Fig. 4.

Figure 5 shows the current efficiency and hydrogen content of nickel films obtained at pH = 1.5 as a function of solution temperature. The current efficiency at 20°C is quite small, but becomes higher with increasing solution temperature. The corresponding hydrogen content indicates that the low current efficiency is accompanied by the incorporation of more hydrogen. The general correlation between two curves is that the higher the hydrogen content, the lower the current efficiency for nickel deposition.

Figure 6 shows the results of a ductility test on films A, B, and C. The results indicate the probable existence of maximum ductility around 50°C. Furthermore, the film ductility at 20°C is similar to that at 100°C. The trend of the curve appears to be related to the microstructures shown in Fig. 2.

Nickel deposits from a high pH (5.8) solution.—Contrary to the low pH case, nickel films deposited from the high pH (5.8) solution did not show the large structural and ductility variation with solution temperatures. The use of the high resolution defocus contrast technique, however, revealed that a high density of small (~10Å) inclusions (probably hydroxides) were present in all the films. A nickel film obtained at 20°C is shown in Fig. 7. Two black arrows mark the images of inclusions taken in the slightly underfocused condition. The density of these inclusions was found to be generally less at higher temperatures. Figure 8 then qualitatively shows that the incorporation of inclusions is associated with a reduction in the current efficiency.

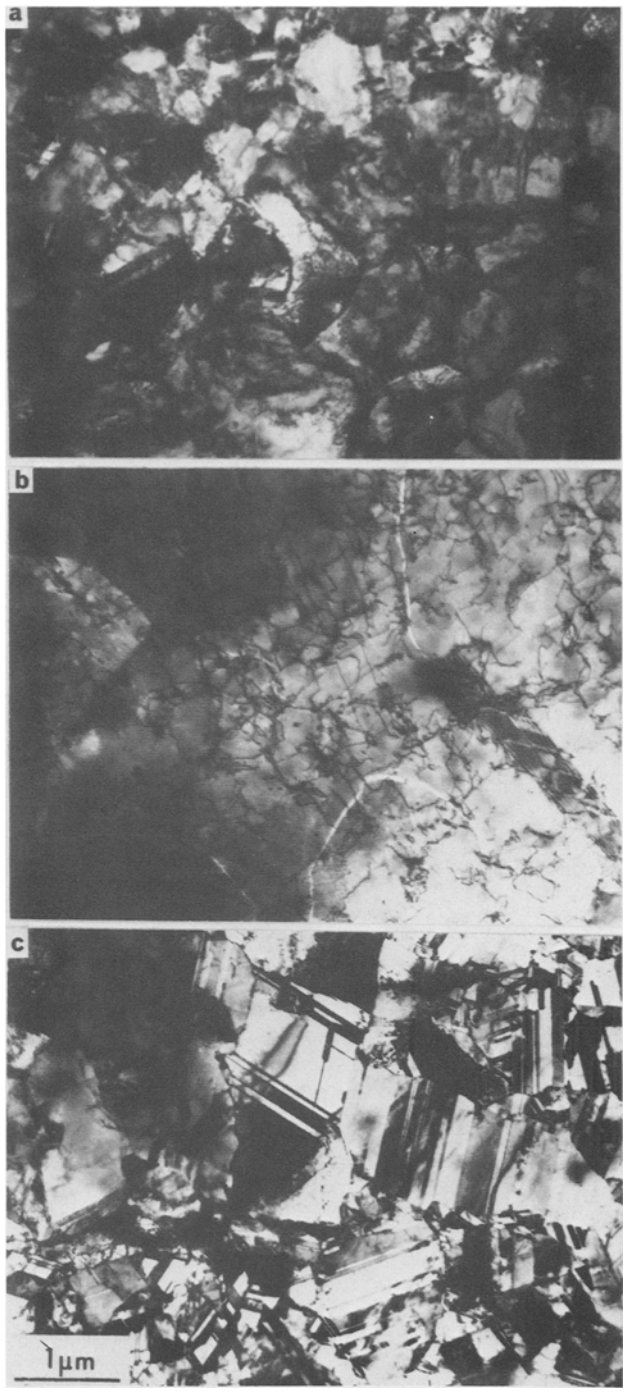

Fig. 2. Microstructures of nickel films obtained in the low pH (1.5) solution at (a) 20°, (b) 50°, and (c) 100°C.

Discussion

It has been shown how incorporation of hydrogen or probable hydroxide affects the microstructure and ductility of nickel electrodeposits. Since the degree of this incorporation depends strongly on solution pH and temperature, the microstructure and ductility follow these two variables accordingly. As evidenced by previous electrochemical studies (1-5), the inclusion of hydrogen or hydroxide decreases with increasing solution temperature. The results from the current efficiency and chemical analysis indeed support this trend. It is clear that the solution pH changes the type of foreign species and the degree of their adsorption. The important result here is that similar to the cobalt case, deposition at low pH and low temperature has a

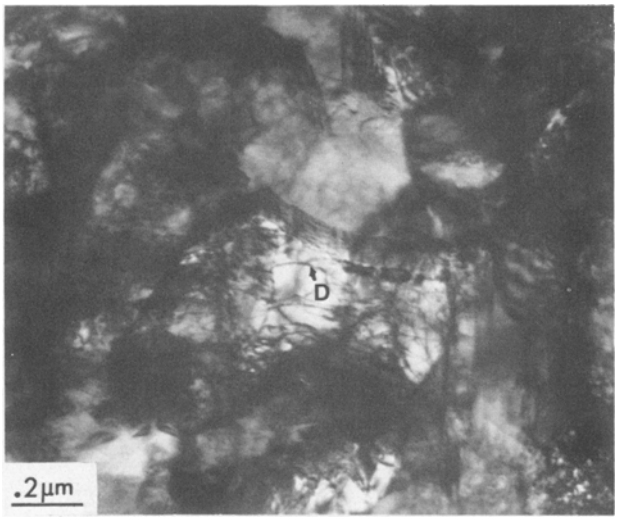

Fig. 3. A high density of dislocations in a nickel film obtained in the low pH (1.5) solution at 20°C. The symbol, D, denotes a segment of dislocation apparently generated by plastic deformation.

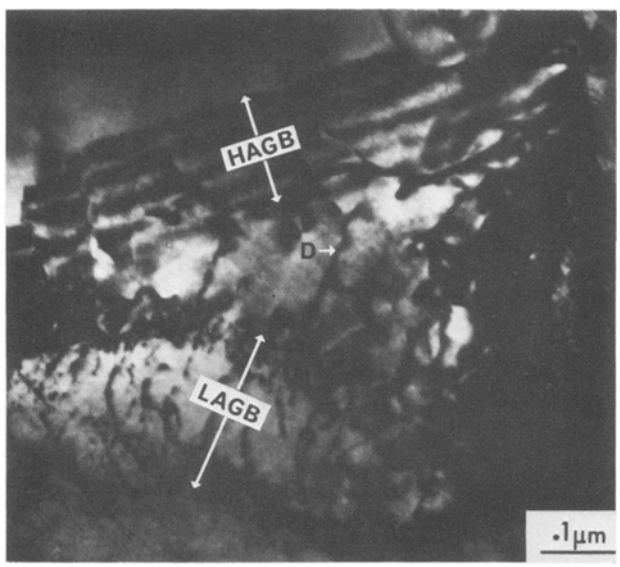

Fig. 4. A high density of dislocations forming a low angle grain boundary (LAGB) near the high angle grain boundary (HAGB) of a nickel film obtained at low (1.5) pH and 20°C.

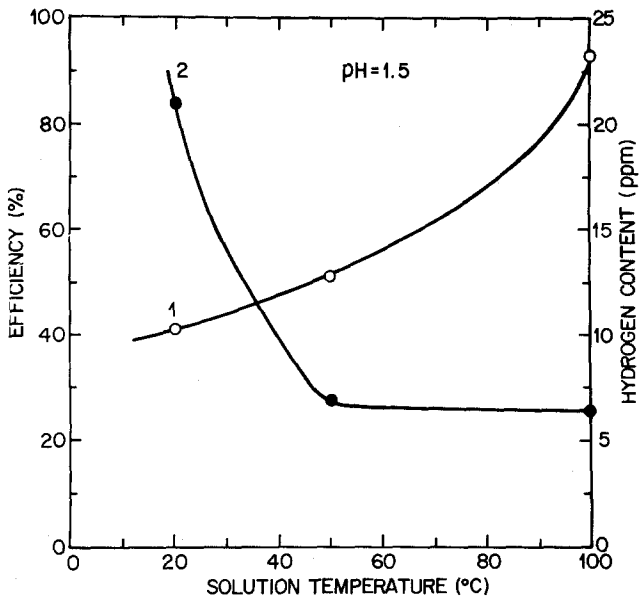

Fig. 5. Effect of solution temperature on the current efficiency (curve 1) and hydrogen content (curve 2) of nickel films obtained at pH = 1.5.

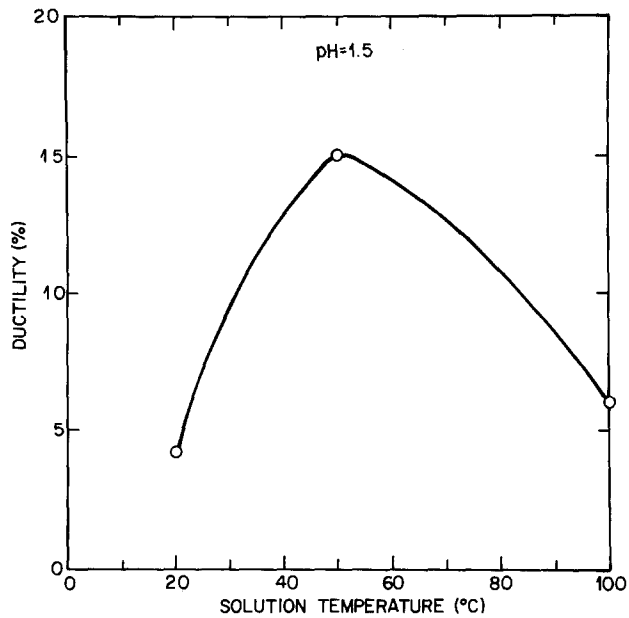

Fig. 6. Ductility of nickel films at pH = 1.5 plotted as a function of solution temperature.

dramatic effect on the nickel microstructure, *i.e.*, dislocation structure.

The presence of a high density of dislocations in nickel films obtained at low *p*H and low temperature can be explained by the formation of unstable nickel hydride during film growth. As noted in the chemical analysis and current efficiency, such a low current efficiency (40% at *p*H = 1.5 and 20°C) strongly suggests that a considerable amount of hydrogen evolves at a cathode in this *p*H and temperature range, and this deposition mode apparently resembles a cathodic charging process. Nonstoichiometric nickel hydride NiH_n (n = 0.1-0.9) was previously found (11) to be formed in cathodically charged nickel. Nickel hydride, obtained by charging, has the fcc structure with the lattice parameter about 6% larger than that of pure nickel. Although the nickel hydride phase does exist, it is unstable at ambient temperatures. Further study (12) on this phase indicates that the nickel hydride exists in the form of both alpha and beta phases. In order to check these results, we have conducted a hydrogen charging experiment on an annealed bulk nickel foil in a 1*N* H_2SO_4 solution at 200 mA/cm² for 1 min. It was found that the originally almost dislocation-free foil was transformed into a highly defected one. In fact, the dislocation density was too large to be measured quantitatively.

From the above evidence, it is reasonable to assume that the unstable nickel hydride initially forms during the deposition in low *p*H and low temperature solution, but rapidly decomposes at ambient temperature. During this decomposition process, a plastic deformation equivalent to 6% plastic strain will occur in the films, resulting in the formation of the numerous slip dislocations observed. It is apparent that such a structural transformation involves only fcc to fcc structure and thus the faulting observed in cobalt during the fcc → hcp transformation is not expected, but the formation of dislocations occurs. This is indeed the case in the present results. This process is schematically shown in Fig. 9. Although the earlier electron diffraction study by Yang (13) indicated the existence of hcp nickel possibly containing hydrogen, the absence of stacking faults in our films rules out such a possibility. Nevertheless, the important point here is

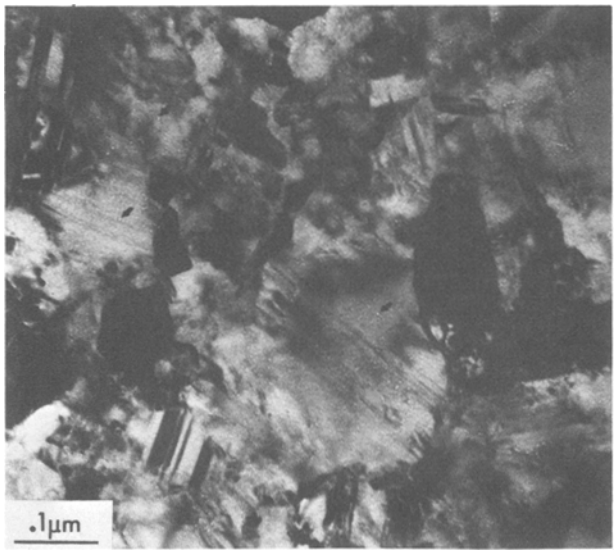

Fig. 7. Microstructure of a nickel film obtained at pH = 5.8 and 20°C. Three arrows indicate the images (white dots) of probable hydroxide inclusions.

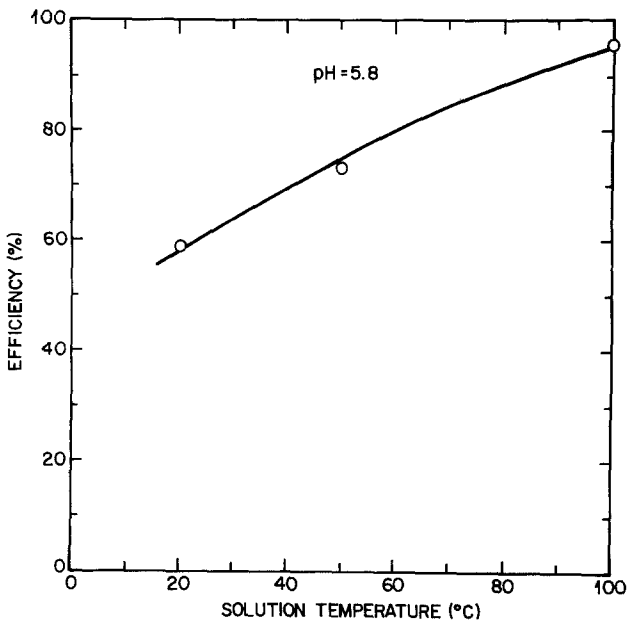

Fig. 8. Current efficiency plotted as a function of solution temperature for nickel films obtained at pH = 5.8.

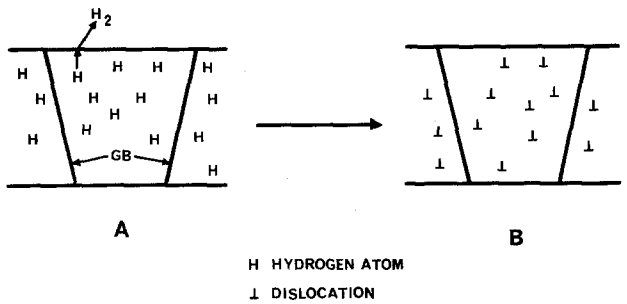

Fig. 9. A schematic diagram showing how plastic deformation occurs by the outdiffusion of hydrogen atoms incorporated in nickel films deposited at low (1.5) pH and low solution temperature.

that the incorporation of hydrogen has a marked effect on the microstructure of iron-group metals.

It is evident from the present proposition that the hydrogen content of the deposits only qualitatively describes the amount actually incorporated inside the deposits, since the major portion must have diffused out of the films during the decomposition of nickel hydride. Since the trend of the current efficiency as a function of solution temperature appears to follow reciprocally that of the hydrogen content, it is reasonable to assume that the remaining hydrogen content is proportional to the amount actually incorporated prior to the decomposition. The remaining hydrogen in the deposits is probably contained inside small voids which are commonly observed in electrodeposited films.

The observed ductility maximum (see Fig. 6) in the nickel films deposited at low pH solution can be explained by the grain size. At the low temperature, the adsorption of hydrogen inhibits the growth of nickel and thus produces small (0.5 ~ 1 μm) grains. Due to the presence of low angle grain boundaries induced by the plastic deformation, the effective grain size becomes somewhat smaller than the above size. At the intermediate temperature (50°C), the inhibition becomes smaller and, consequently, nickel grows to the larger (6 ~ 20 μm) size. At high temperature (100°C), however, a further decrease in this inhibition brings about a higher nickel deposition rate, as evidenced by the increased current efficiency (see Fig. 5). The increased deposition rate produces a higher nucleation rate, resulting in grain refinement. The film ductility can therefore be explained by the grain size variation. The maximum in film ductility at 50°C is due to the large grain size. Similar observations have previously been made by Zhamagortsyan *et al.* (5) on the microhardness and internal stress of nickel films prepared in a similar manner to the present work. Although they did not conclusively explain this phenomenon in terms of the grain size variation, it is clear that their microhardness and internal stress can be attributed to the same origin as our ductility result.

It is important to point out here that the reduction in the grain size of nickel films obtained at low pH (1.5) and high temperature (100°C) is accompanied by the formation of numerous growth twins [see Fig. 2(c)]. In this pH and temperature range, the increased nickel deposition rate causes the high probability of making 111 stacking (ABCABCABC . . .) mistakes on {111} growth faces, resulting in the formation of numerous growth twins.

The effect of probable hydroxide inclusions on the nickel microstructures seen in the high pH solution resembles that of an addition agent. Besides altering the grain size, the hydroxide inclusions do not appear to contribute to the formation of dislocations as is the case for hydrogen. In contrast to the extreme case where epitaxial hydroxides are formed in an unbuffered solution (14), the observed hydroxide inclusions were in a more colloidal form and were likely to be trapped on growth steps during film formation. We found from an electron diffraction analysis that these inclusions are amorphous.

Conclusions

It has been shown that the incorporation of hydrogen and hydroxide alters the nickel microstructure significantly. This observation is indeed consistent with previous electrochemical results and the microstructural observations on electrodeposits of the other iron-group metal, cobalt. Since the incorporation depends strongly on the degree of adsorption, the resulting microstructure depends on the solution pH and temperature. It is clear from these observations that the inhibition effect is intrinsically high in the deposition of iron-group metals. Care should thus be taken if one wishes to study an additional inhibition affect from an addition agent.

Manuscript submitted April 14, 1981; revised manuscript received June 30, 1981.

Any discussion of this paper will appear in a Discussion Section to be published in the December 1982

JOURNAL. All discussions for the December 1982 Discussion Section should be submitted by Aug. 1, 1982.

Publication costs of this article were assisted by Bell Laboratories.

REFERENCES

1. A. T. Vagramyan and Yu. S. Petrova, "The Mechanical Properties of Electrolytic Deposits," Consultants Bureau, New York (1960).
2. A. T. Vagramyan and L. A. Uvarov, *Izv. Akad. Nauk. SSSR Otd. Khim.*, **9**, 1520 (1962).
3. A. T. Vagramyan, M. A. Zhamagortsyan, and L. A. Uvarov, *Izv. Akad. Nauk. SSSR Ser. Khim.*, **2**, 301 (1964).
4. Yu. P. Balakin, A. T. Vagramyan, and L. A. Uvarov, *ibid.*, **3**, 398 (1966).
5. M. A. Zhamagortsyan, Z. N. Pilikyan, A. A. Yavich, and A. T. Vagramyan, *Elektrokhimiya*, **11**, 437 (1975).
6. J. G. Wright and J. Goddard, *Philos. Mag.*, **14**, 485 (1965).
7. J. G. Wright, *Thin Solid Films*, **22**, 197 (1974).
8. S. Nakahara and S. Mahajan, *This Journal*, **127**, 283 (1980).
9. S. Nakahara and Y. Okinaka, in "Properties of Electrodeposits—Their Measurements and Significance," R. Sard, H. Leidheiser, Jr., and F. Ogburn, Editors, Chap. 3, The Electrochemical Society Softbound Proceedings Series, Princeton, NJ (1975).
10. S. Nakahara, Y. Okinaka, and D. R. Turner, *J. Testing Evaluation*, **5**, 178 (1977).
11. A. Janko, *Naturwissenschaften*, **47**, 225 (1960).
12. S. Majchrzak, *Bull. Acad. Pol. Sci., Ser. Sci. Chim.*, **15**, 485 (1967).
13. L. Yang, *This Journal*, **97**, 241 (1950).
14. A. G. Ives, J. W. Edington, and G. P. Rothwell, *Electrochim. Acta*, **15**, 1797 (1970).

Current-Induced Composition Gradients in Molten $AgNO_3$-$NaNO_3$: A Model System for the LiCl-KCl Electrolyte of an Li/S Battery

C. E. Vallet* and D. E. Heatherly

Oak Ridge National Laboratory, Chemistry Division, Oak Ridge, Tennessee 37830

R. L. Sherman

Oak Ridge National Laboratory, Analytical Chemistry Division, Oak Ridge, Tennessee 37830

and J. Braunstein*

Oak Ridge National Laboratory, Chemistry Division, Oak Ridge, Tennessee 37830

ABSTRACT

Composition gradients, in molten $AgNO_3$-$NaNO_3$ mixtures contained in silica frits, are produced by electrolysis between silver electrodes and analyzed by three methods: (*i*) *in situ* potentiometry, (*ii*) chemical analysis of sections of quenched electrolyte, and (*iii*) scanning electron microscopy with associated x-ray fluorescence spectroscopy. The composition changes are calculated *a priori* from transport and thermodynamic properties independently measured in the free melt and corrected for the porosity of the frits. Since the ion flows in $AgNO_3$-$NaNO_3$ are analogous to those in the LiCl-KCl electrolyte of Li/S batteries, the former system serves as a convenient model system for the mixed electrolyte of the Li/S battery. The predicted gradients are compared to the experimental data from the three methods.

Binary and multicomponent mixtures of molten salts are used as the electrolyte in some high temperature batteries (1). At typical current densities, composition changes within the electrolyte may arise from the electrode reactions and ionic migration. Our previous analysis (2) of diffusive and migrational transport in binary molten salt mixtures predicted significant concentration gradients in two-component melts. Recent more complex model calculations (3), which include effects of forced convection, temperature, and electrode porosity, predict similar gradients. Composition gradients of the predicted magnitude were measured at the electrodes by *in situ* potentiometry and by chemical analysis of $AgNO_3$-KNO_3 electrolyzed between silver electrodes, a system in which the ion flows are analogous to those in an Li/LiCl-KCl/FeS_x battery (4). A quantitative test of models requires both a system in which the thermodynamic and transport properties are better known and detailed measurements of the composition profiles.

In this paper, we present new measurements of electrolysis-induced composition changes in $AgNO_3$-$NaNO_3$ contained in silica frits. For this system the diffusion coefficient (5), the transference number (6, 7), and the activity coefficient (8), are independently known. Correction for the tortuosity of the path for diffusion and conduction is made from measurements of the frit porosity and electrical conductance. In addition to potentiometry and chemical analysis, the composition profiles in the quenched mixture are measured with high resolution of distance by scanning electron microscopy and associated x-ray fluorescence spectroscopy (SEM/EDX). The SEM/EDX results are consistent with the data from chemical analysis and from *in situ* potentiometric measurements. The results from the three kinds of experiments are compared to predictions calculated with no adjustable parameters.

* Electrochemical Society Active Member.
Key words: migration, diffusion, fused salts, battery, SEM.